M2AN - MODÉLISATION MATHÉMATIQUE ET ANALYSE NUMÉRIQUE

SOPHIE DEPEYRE
DIDIER ISSAUTIER

A new constrained formulation of the Maxwell system

M2AN - Modélisation mathématique et analyse numérique, tome 31, n° 3 (1997), p. 327-357

<http://www.numdam.org/item?id=M2AN_1997__31_3_327_0>

© AFCET, 1997, tous droits réservés.

L'accès aux archives de la revue « M2AN - Modélisation mathématique et analyse numérique » implique l'accord avec les conditions générales d'utilisation (http://www.numdam.org/conditions). Toute utilisation commerciale ou impression systématique est constitutive d'une infraction pénale. Toute copie ou impression de ce fichier doit contenir la présente mention de copyright.

NUMDAM
Article numérisé dans le cadre du programme
Numérisation de documents anciens mathématiques
http://www.numdam.org/

MATHEMATICAL MODELLING AND NUMERICAL ANALYSIS
MODÉLISATION MATHÉMATIQUE ET ANALYSE NUMÉRIQUE

(Vol 31, n° 3, 1997, p 327 à 357)

A NEW CONSTRAINED FORMULATION OF THE MAXWELL SYSTEM (*)

Sophie DEPEYRE (1), Didier ISSAUTIER (1, 2)

Abstract — *We present in this paper a new constrained formulation of the Maxwell equations in order to improve the numerical verification of the divergence relations* div $\mathbf{B} = 0$, div $\mathbf{E} = \frac{\rho}{\epsilon_0}$ *We prove, using the modified equations, why these relations are better satisfied by considering this new formulation. We also study the stability of the presented schemes*

Résumé — *Nous présentons dans ce papier une nouvelle formulation des équations de Maxwell afin de mieux vérifier numériquement les relations de divergence* div $\mathbf{B} = 0$, div $\mathbf{E} = \frac{\rho}{\epsilon_0}$. *Nous montrerons, en établissant les équations équivalentes, pourquoi ces relations sont mieux vérifiées en considérant cette nouvelle formulation Nous avons également étudié la stabilité des schémas présentés*

INTRODUCTION

We are concerned, in this paper, with the divergence conditions for the electromagnetic field. The electric field must satisfy Gauss law and the magnetic field must be divergence free. Using the charge conservation equation, these conditions are redundant in the continuous model and then are not considered at the discrete level. Some methods, like finite difference or finite volume schemes, satisfy these conditions but require the use of a cartesian grid or a dual grid. Nevertheless, this redundance is generally no more observed in the discrete model. In the case of unstructured meshes, we have observed that these conditions were not exactly satisfied and that the error depended on the mesh step and on the space accuracy of the scheme [5]. More precisely, this error seems to depend on the numerical viscosity of the schemes used. Without charges, the different test cases considered in [5] have proved that this error did not have an important influence on the accuracy of the solution for meshes with 15 to 20 points per wavelength. The satisfaction of these conditions would allow to reduce the number of mesh nodes and then would increase the efficiency of the solver especially in the three-dimensional simulations case.

(*) Manuscript received July 25, 1995

(1) CERMICS-INRIA, 2004, route des Lucioles, B P 93, 06902 Sophia-Antipolis Cedex

(2) Laboratoire J -A. Dieudonné, U.R A 168 du CNRS Université de Nice Sophia-Antipolis Parc Valrose, BP 71, 06108 Nice Cedex 02.

M^2 AN Modélisation mathématique et Analyse numérique 0764-583X/97/03/$ 7 00
Mathematical Modelling and Numerical Analysis © AFCET Gauthier-Villars

In the case of charged media, the satisfaction or not of these conditions has a great influence on the accuracy of the solution. A convenient way to deal with this problem is to introduce the Lagrange multipliers associated with the divergence conditions [1]. Our approach is quite different, we propose a new constrained formulation of the Maxwell system in order to better satisfy the divergence conditions.

The paper is divided into six parts. In the first two parts, we present the Maxwell equations and the numerical approximation used. In the third part, we present the constrained formulation of the Maxwell system. In the next two parts, we prove using a stability analysis and the modified equations, why the divergence conditions are better satisfied by considering this new formulation. Finally we present some numerical results in order to demonstrate the efficiency of this method.

1. MAXWELL EQUATIONS

We introduce the Maxwell equations :

$$\begin{cases} \dfrac{\partial \mathbf{E}}{\partial t} - c^2 \operatorname{rot}(\mathbf{B}) = -\dfrac{\mathbf{j}}{\epsilon_0} & (1.1) \\ \dfrac{\partial \mathbf{E}}{\partial t} + \operatorname{rot}(\mathbf{E}) = 0 & (1.2) \\ \operatorname{div}(\mathbf{E}) = \dfrac{\rho}{\epsilon_0} & (1.3) \\ \operatorname{div}(\mathbf{B}) = 0 & (1.4) \end{cases}$$

where $\mathbf{E} = \mathbf{E}(t, \mathbf{x})$ is the electric field and $\mathbf{B} = \mathbf{B}(t, \mathbf{x})$ is the magnetic field induction. c is the speed of the light in the vacuum, ϵ_0 is the dielectric permittivity in the vacuum and μ_0 is the magnetic permeability in the vacuum. These values are coupled by the relation : $\epsilon_0 \mu_0 c^2 = 1$.

The charge density $\rho = \rho(t, \mathbf{x})$ and the current density $\mathbf{j} = \mathbf{j}(t, \mathbf{x})$ are related by the conservation equation :

$$\frac{\partial \rho}{\partial t} + \operatorname{div}(\mathbf{j}) = 0 . \qquad (2)$$

It is well known that the constraints $\operatorname{div} \mathbf{E} = \dfrac{\rho}{\epsilon_0}$ and $\operatorname{div} \mathbf{B} = 0$ are satisfied at any time t for initial conditions verifying these relations.

2. NUMERICAL APPROXIMATION

The Maxwell system is of hyperbolic type and is also a law-conservation system. These characteristics lead up to a numerical approximation based on a finite volume method.

2.1. Conservative form and hyperbolicity

The Maxwell equations (1.1) and (1.2) can be written in the following form :

$$\mathbf{Q}_t + \mathbf{F}_1(\mathbf{Q})_x + \mathbf{F}_2(\mathbf{Q})_x + \mathbf{F}_3(\mathbf{Q})_x = \mathbf{J} \tag{3}$$

where :

$$\begin{cases} \mathbf{Q} = {}^t(E_1, E_2, E_3, B_1, B_2, B_3) \\ \mathbf{F}_1(\mathbf{Q}) = {}^t(0, c^2 B_3, -c^2 B_2, 0, -E_3, E_2) \\ \mathbf{F}_2(\mathbf{Q}) = {}^t(-c^2 B_3, 0, c^2 B_1, E_3, 0, -E_1) \\ \mathbf{F}_3(\mathbf{Q}) = {}^t(c^2 B_2, -c^2 B_1, 0, -E_2, E_1, 0) \\ \mathbf{J} = -\dfrac{1}{\epsilon_0}{}^t(j_1, j_2, j_3, 0, 0, 0) . \end{cases}$$

Let us write (3) as :

$$\mathbf{Q}_t + \vec{\nabla} \cdot \mathbb{F}(\mathbf{Q}) = \mathbf{J} \tag{4}$$

with $\mathbb{F}(\mathbf{Q}) = {}^t(\mathbf{F}_1(\mathbf{Q}) ; \mathbf{F}_2(\mathbf{Q}) ; \mathbf{F}_3(\mathbf{Q}).)$

We now consider the following linear combination $\mathscr{F}(\mathbf{Q}, \boldsymbol{\eta}) = \boldsymbol{\eta} \cdot \mathbb{F}(\mathbf{Q})$ where $\boldsymbol{\eta} = (\eta_1, \eta_2, \eta_3)$ is any non-zero constant vector in $\mathbb{R}^3$. The jacobian matrix $\mathscr{A}$ defined by :

$$\mathscr{A}(\mathbf{Q}, \boldsymbol{\eta}) = \boldsymbol{\eta} \cdot \mathbb{F}'(\mathbf{Q}) = \eta_1 \mathscr{A}_1 + \eta_2 \mathscr{A}_2 + \eta_3 \mathscr{A}_3 ,$$

$$(\mathscr{A}_i)_{i=1, \ldots, 3} = \frac{\partial}{\partial(\mathbf{Q})} \mathbf{F}_i(\mathbf{Q})$$

is diagonalizable for all non-zero vector in $\mathbb{R}^3$ and for all vector $\mathbf{Q}$ in $\mathbb{R}^6$.

Its three real eigenvalues with double multiplicity are given by :

$$\begin{cases} \lambda_1 = c \| \boldsymbol{\eta} \| \\ \lambda_2 = -c \| \boldsymbol{\eta} \| \\ \lambda_3 = 0 . \end{cases}$$

This property of Maxwell system leads up naturally to the use of upwind schemes which are known to be well adapted to solve numerically hyperbolic conservative systems. We are interested, in this paper, in high order upwind schemes both in time and space using structured and unstructured grids.

2.2. Weak formulation

Let $\mathcal{T}_h$ be a standard finite element discretization of Ω_h, the polygonal approximation (tetrahedron or parallelepiped) of a computational domain Ω At each node S_i, a cell C_i is constructed as shown in figure 1 The union of all the cells forms a new partition of Ω_h

$$\Omega_h = \bigcup_{i=1}^{ns} C_i$$

where ns is the number of mesh nodes

We consider the Cauchy problem

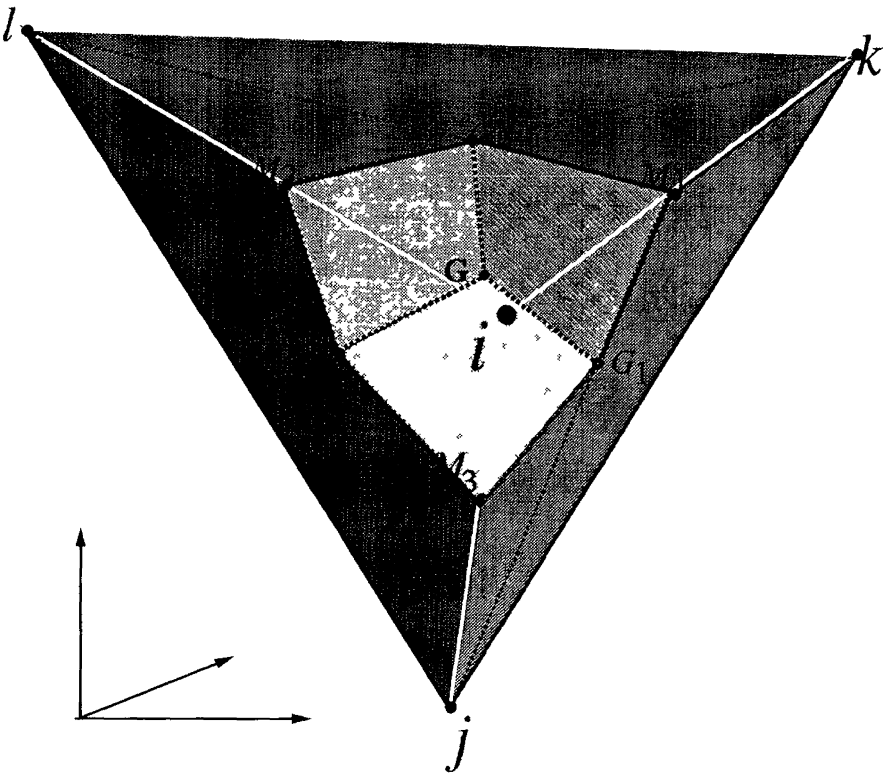

Figure 1. — Cell construction for meshes in tetrahedra.

$$\begin{cases} \mathbf{Q}_t + \vec{\nabla} \cdot \mathbb{F}(\mathbf{Q}) = \mathbf{J} & (\mathbf{x}, t) \in \Omega \times \mathbb{R}^+ \\ \mathbf{Q}(\mathbf{x}, t = 0) = \mathbf{Q}_0(\mathbf{x}) & \mathbf{x} \in \Omega \end{cases} \tag{6}$$

where $\mathbf{Q}_0$ satisfies the divergence conditions (1.3) and (1.4). We complete (6) with appropriate boundary conditions.

The weak formulation of (6) writes, for each cell C_i, as :

$$\int_{C_i} (\mathbf{Q}_t + \vec{\nabla} \cdot \mathbb{F}(\mathbf{Q})) \, d\mathbf{x} = \int_{C_i} \mathbf{J} \, d\mathbf{x} . \tag{7}$$

Assuming partial derivative $\mathbf{Q}_t$ to be constant in space on C_i and using a Green formula leads to :

$$Vol(C_i) (\mathbf{Q}_t)_i + \sum_{j \in K(i)} \int_{\partial C_{ij}} \mathbb{F}(\mathbf{Q}) \cdot \nu_{ij} \, d\sigma = \int_{C_i} \mathbf{J} \, d\mathbf{x} \tag{8}$$

where ν_{ij} is the outward unit normal to the interface ∂C_{ij} between two cells C_i and C_j, and $K(i)$ is the set of the neighbouring nodes of the node S_i.

2.3. First-order upwind flux

We describe the approximation of the flux $\int_{\partial C_{ij}} \mathbb{F}(\mathbf{Q}) \cdot \nu_{ij} \, d\sigma$. To evaluate this integral, we introduce the notation :

$$\eta = \int_{\partial C_{ij}} \nu_{ij} \, d\sigma .$$

We choose an upwind approximation for the numerical fluxes Φ_{ij}. Using Steger-Warming flux splitting, the numerical fluxes are written :

$$\Phi_{ij} = \Phi(\mathbf{Q}_i, \mathbf{Q}_j, \eta) = \mathscr{A}^+ \mathbf{Q}_i + \mathscr{A}^- \mathbf{Q}_j \tag{9}$$

where $\mathscr{A}^+$ and $\mathscr{A}^-$ denote the positive and negative parts respectively of $\mathscr{A}$. We refer to [6] for the treatment of the boundary conditions.

2.4. High-order approximation

We construct now a third-order accurate scheme in space using the extension of Van Leer's MUSCL (Monotonic Upwind Schemes for Conservation Laws) method to finite elements [9]. One way to achieve high-order accuracy is to increase the degree of the interpolation of the solution in a cell and to

evaluate the fluxes with some extrapolated values $\mathbf{Q}_{ij}$ and $\mathbf{Q}_{ji}$ at the cell interface ∂C_{ij}. In the MUSCL method, these values are obtained by a linear interpolation on each cell. We use here a formulation, called β-scheme, to define the values $\mathbf{Q}_{ij}$ and $\mathbf{Q}_{ji}$ at the cell interface :

$$\begin{cases} \Phi_{ij} = \Phi_{ij}(\mathbf{Q}_{ij}, \mathbf{Q}_{ji}) \\ \mathbf{Q}_{ij} = \mathbf{Q}_i + \frac{1}{2}\{(1-2\beta)(\mathbf{Q}_j - \mathbf{Q}_i) + 2\beta \vec{\nabla}\mathbf{Q}_i^H . \mathbf{S}_i \mathbf{S}_j\} \\ \mathbf{Q}_{ji} = \mathbf{Q}_j - \frac{1}{2}\{(1-2\beta)(\mathbf{Q}_j - \mathbf{Q}_i) + 2\beta \vec{\nabla}\mathbf{Q}_j^H . \mathbf{S}_i \mathbf{S}_j\} \end{cases} \tag{10}$$

where β is an upwinding parameter which determines the accuracy of the scheme. If we take $\beta = \frac{1}{3}$, we achieve a quasi third-order scheme in space for unstructured meshes. In the case of structured meshes, this scheme is exactly third-order accurate [8].

This extension requires the evaluation of the gradient of the solution at each node. The nodal gradients may be defined in several ways. We use here the following definition :

— For meshes made of parallelepiped :

$$\vec{\nabla}\mathbf{Q}_{iR}^H = \frac{1}{Vol(Supp(\varphi_i))} \int_{Supp(\varphi_i)} \vec{\nabla}\mathbf{Q}\, dx$$

$$= \frac{1}{Vol(Supp(\varphi_i))} \sum_{R,\, i \in R} \sum_{k=1}^{8} \mathbf{Q}_k \int_R \vec{\nabla}\varphi_k\, dx \tag{11}$$

where S_k $(k = 1, ..., 8)$ are the eight nodes of the parallelepiped R and $\vec{\nabla}\varphi_k$ is the gradient of the Q1 basis function associated to the node S_k.

— For meshes made of tetrahedra :

$$\vec{\nabla}\mathbf{Q}_{iT}^H = \frac{1}{Vol(Supp(\varphi_i))} \int_{Supp(\varphi_i)} \vec{\nabla}\mathbf{Q}\, dx$$

$$= \frac{1}{Vol(C_i)} \sum_{T,\, i \in T} \frac{Vol(T)}{3} \sum_{k=1}^{4} \mathbf{Q}_k\, \vec{\nabla}\varphi_k^T \tag{12}$$

where S_k $(k = 1, 2, 3, 4)$ are the four vertices of the tetrahedron T and $\vec{\nabla}\varphi_k(T)$ is the constant gradient on T of the P1 basis function associated to the node S_k.

2.5. Time integration

We need an accurate time integration scheme when dealing with unstationary problems. We use here explicit Runge-Kutta schemes with r steps and low storage :

$$\begin{cases} Q^0 = Q^n \\ Q^l = Q^0 - \dfrac{\Delta t}{(r+1-l)}\,\Phi(Q^{l-1}) \quad l = 1, 2, ..., r \\ Q^{n+1} = Q^r \end{cases}$$

where $t^n = n\,\Delta t$ and $\Phi(\mathbf{Q}^{l-1})$ represent the fluxes calculated with fields $\mathbf{Q}^{l-1}$. In the case $r = 3$, this scheme is third-order in time because the Maxwell system is linear.

3. A CONSTRAINED FORMULATION FOR THE MAXWELL EQUATIONS

3.1. The Maxwell equations as a constrained problem

In practice, the numerical approximation of the charge and current densities ρ and $\mathbf{j}$ do not exactly satisfy the charge conservation law (2) and consequently the divergence conditions (1.3) and (1.4) are not satisfied.

A convenient way to deal with this problem is to introduce the Lagrange multipliers of the constraints (1.3) and (1.4). However this leads to solve a Laplace equation at each time step [1].

We prefer to use here a viscosity approach which is more related to the numerical scheme we use. Let $\bar{\alpha}$ and $\bar{\gamma}$ (in s/m^2) denote two positive constants, we consider the new problem :

$$\begin{cases} \dfrac{\partial \mathbf{E}}{\partial t} - c^2\,\mathrm{rot}\,(\mathbf{B}) - \dfrac{1}{\bar{\alpha}}\nabla\left(\mathrm{div}\,\mathbf{E} - \dfrac{\rho}{\epsilon_0}\right) = -\dfrac{1}{\epsilon_0}\mathbf{j} & (13.1) \\ \dfrac{\partial \mathbf{B}}{\partial t} + \mathrm{rot}\,(\mathbf{E}) - \dfrac{1}{\bar{\gamma}}\nabla\,(\mathrm{div}\,\mathbf{B}) = 0 & (13.2) \end{cases}$$

Concerning the system (13.1, 13.2), we have the following results :

PROPOSITION 3.1 : *Systems (1.1, 1.2) and (13.1, 13.2) are equivalents if the initial conditions* $\mathbf{E}_0$, $\mathbf{B}_0$ satisfy (3).

PROPOSITION 3.2 : *This new formulation (13.1, 13.2) of the Maxwell equations preserves the energy estimates.*

We refer to [11] for a proof of these propositions.

System (13.1, 13.2) writes in dimensionless variables as :

$$\begin{cases} \dfrac{\partial \mathbf{E}}{\partial t} - \text{rot}\,(\mathbf{B}) - \dfrac{1}{\alpha}\nabla\,(\text{div}\,\mathbf{E} - \rho) = -\,\mathbf{j} & (13.3) \\ \dfrac{\partial \mathbf{B}}{\partial t} + \text{rot}\,(\mathbf{E}) - \dfrac{1}{\gamma}\nabla\,(\text{div}\,\mathbf{B}) = 0\,. & (13.4) \end{cases}$$

We observe that taking the divergence of (13.3, 13.4) leads to a heat equation for the divergence constraints, [11].

3.2. Weak formulation

Equations (13.3, 13.4) can be written in the following form :

$$\mathbf{Q}_t + \mathbf{F}_1(\mathbf{Q})_x + \mathbf{F}_2(\mathbf{Q})_y + \mathbf{F}_3(\mathbf{Q})_x = \mathbf{J} + \mathbf{G}_1(\mathbf{Q})_x + \mathbf{G}_2(\mathbf{Q})_y + \mathbf{G}_3(\mathbf{Q})_x \quad (14)$$

where :

$$\begin{cases} \mathbf{Q} = {}^t(E_1, E_2, E_3, B_1, B_2, B_3) \\ \mathbf{F}_1(\mathbf{Q}) = {}^t(0, B_3, -B_2, 0, -E_3, E_2) \\ \mathbf{F}_2(\mathbf{Q}) = {}^t(-B_3, 0, B_1, E_3, 0, -E_1) \\ \mathbf{F}_3(\mathbf{Q}) = {}^t(B_2, -B_1, 0, -E_2, E_1, 0) \\ \mathbf{J} = -\,{}^t(j_1, j_2, j_3, 0, 0, 0) \\ \mathbf{G}_1(\mathbf{Q}) = {}^t\Big(\dfrac{1}{\alpha}(\text{div}\,\mathbf{E} - \rho), 0, 0, \dfrac{1}{\gamma}\,\text{div}\,\mathbf{B}, 0, 0\Big) \\ \mathbf{G}_2(\mathbf{Q}) = {}^t\Big(0, \dfrac{1}{\alpha}(\text{div}\,\mathbf{E} - \rho), 0, 0, \dfrac{1}{\gamma}\,\text{div}\,\mathbf{B}, 0\Big) \\ \mathbf{G}_3(\mathbf{Q}) = {}^t\Big(0, 0, \dfrac{1}{\alpha}(\text{div}\,\mathbf{E} - \rho), 0, 0, \dfrac{1}{\gamma}\,\text{div}\,\mathbf{B}\Big)\,. \end{cases}$$

Using the notations introduced previously, a weak formulation of (13) is :

$$\int_{C_i} (\mathbf{Q}_t + \mathbf{F}_1(\mathbf{Q})_x + \mathbf{F}_2(\mathbf{Q})_y + \mathbf{F}_3(\mathbf{Q})_x)\,d\mathbf{x} =$$

$$\int_{C_i} \mathbf{J}\,d\mathbf{x} + \int_{C_i} (\mathbf{G}_1(\mathbf{Q})_x + \mathbf{G}_2(\mathbf{Q})_y + \mathbf{G}_3(\mathbf{Q})_x)\,d\mathbf{x}$$

Using a Green formula leads to :

$$\int_{C_i} \mathbf{Q}_i \, d\mathbf{x} + \int_{\partial C_i} (\mathbf{F}_1 \, \nu_{ix} + \mathbf{F}_2 \, \nu_{iy} + \mathbf{F}_3 \, \nu_{ix}) \, d\sigma =$$

$$\int_{C_i} \mathbf{J} \, d\mathbf{x} + \int_{\partial C_i} (\mathbf{G}_1 \, \nu_{ix} + \mathbf{G}_2 \, \nu_{iy} + \mathbf{G}_3 \, \nu_{ix}) \, d\sigma$$

We now precise the approximation of the diffusive terms :

$$\int_{\partial C_i} (\mathbf{G}_1 \, \nu_{ix} + \mathbf{G}_2 \, \nu_{iy} + \mathbf{G}_3 \, \nu_{ix}) \, d\sigma \, .$$

Using the definition of $\mathbf{G}_1$, $\mathbf{G}_2$ and $\mathbf{G}_3$, we have to compute the following quantities :

$$\int_{\partial C_i} \operatorname{div} \mathbf{B}\boldsymbol{\nu} \, d\boldsymbol{\sigma}, \quad \int_{\partial C_i} (\operatorname{div} \mathbf{E} - \rho) \, \boldsymbol{\nu} \, d\boldsymbol{\sigma} \, .$$

We restrict to the case of tetrahedra meshes, the same approximation will be used for parallelepiped meshes.

To evaluate these terms, we suppose that $\operatorname{div} \mathbf{B}$ et $\operatorname{div} \mathbf{E} - \rho$ are constant in space on each tetrahedron T of nodes $(S_j)_{j=1, \ldots, 4}$:

$$(\operatorname{div} \mathbf{E} - \rho) \, |_T = \operatorname{div} \mathbf{E}|_T - \rho|_T = \sum_{j=1}^{4} \left(E_1^j \frac{\partial \varphi_j^T}{\partial x} + E_2^j \frac{\partial \varphi_j^T}{\partial y} + E_3^j \frac{\partial \varphi_j^T}{\partial z} \right) - \rho_T$$

where E_i^j denotes the value of the i^{th} component of $\mathbf{E}$ at node S_j, φ_j is the P1 basis function associated to the node S_j and $\rho|_T = \frac{1}{4} \sum_{j=1}^{4} \rho_j$. Finally the approximation of the diffusive terms writes as :

$$\begin{cases} \displaystyle\int_{\partial C_i} \operatorname{div} \mathbf{B}\boldsymbol{\nu} \, d\boldsymbol{\sigma} = \sum_{T, S_i \in T} (\operatorname{div} \mathbf{B})|_T \int_{\partial C_i \cap T} \boldsymbol{\nu} \, d\boldsymbol{\sigma} \\ \displaystyle\int_{\partial C_i} (\operatorname{div} \mathbf{E} - \rho) \, \boldsymbol{\nu} \, d\boldsymbol{\sigma} = \sum_{T, S_i \in T} (\operatorname{div} \mathbf{E} - \rho)|_T \int_{\partial C_i \cap T} \boldsymbol{\nu} \, d\boldsymbol{\sigma} \, . \end{cases}$$

Two-dimensional case.

Two types of wave polarization are particularly interesting in electromagnetism : transverse electric polarizations called **TE** ($\mathbf{E} \, . \mathbf{e} = 0$) and transverse

magnetic polarizations called **TM** ($\mathbf{B}.\mathbf{e}_x = 0$). Indeed, in the two-dimensional case, these polarizations allow the Maxwell system to be splitted according to these two types of polarization. In the **TE** case, system (14) writes as :

$$\mathbf{Q}_t + \mathbf{F}_1(\mathbf{Q})_x + \mathbf{F}_2(\mathbf{Q})_y = \mathbf{J} + \mathbf{G}_1(\mathbf{Q})_x + \mathbf{G}_2(\mathbf{Q})_y \tag{15}$$

with :

$$\begin{cases} \mathbf{Q} = {}^t(E_1, E_2, B_3) \\ \mathbf{F}_1(\mathbf{Q}) = {}^t(0, B_3, E_2) \\ \mathbf{F}_2(\mathbf{Q}) = {}^t(-B_3, 0, -E_1) \\ \mathbf{J} = -{}^t(j_1, j_2, 0) \\ \mathbf{G}_1(\mathbf{Q}) = {}^t\left(\frac{1}{\alpha}(\operatorname{div}\mathbf{E} - \rho), 0, 0\right) \\ \mathbf{G}_2(\mathbf{Q}) = {}^t\left(0, \frac{1}{\alpha}(\operatorname{div}\mathbf{E} - \rho), 0\right). \end{cases}$$

4. STABILITY ANALYSIS

In this section we study the stability of the finite-volume schemes applied to the constrained system (13.3, 13.4) using rectangular and triangular meshes. Concerning the classical Maxwell system (1.1, 1.2), one may find a detailed stability analysis in [4]. For the sake of simplicity we limit our study to the two-dimensional case without charge and current : ($\rho = 0, \mathbf{J} = 0$) and we consider only structured grids. We shall consider first-order accurate schemes and then higher order schemes for which we shall study the effect of the upwinding parameter β on the stability.

This stability analysis is based on a Fourier analysis. Let us set :

$$Q^n_{j,k} = \hat{Q}^n \, e^{i(j\theta_1 + k\theta_2)}$$

with $i^2 = -1$. Then one obtains the following relation :

$$\hat{Q}^{n+1} = G_{\theta_1, \theta_2} \hat{Q}^n$$

where G_{θ_1, θ_2} is the 3×3 amplification matrix which depends on Δt, θ_1, θ_2.

A necessary and sufficient stability condition writes :

$$\rho(G_{\theta_1, \theta_2}) \leq 1 \quad \forall(\theta_1, \theta_2) \in [0, 2\pi]^2, \tag{16}$$

where $\rho(G_{\theta_1,\theta_2})$ is the spectral radius of G_{θ_1,θ_2}.

4.1. First-order accurate schemes

The aim of the stability study concerning the constrained system (13.3, 13.4) is to determine an optimum parameter α_{opt}. This parameter has to minimize the discretization error on the divergence equations and will allow us to choose the same time-step as for the classical Maxwell system. Indeed, the effect of the viscosity term is important concerning the stability of the scheme. More precisely, when the viscosity coefficient $(1/\alpha)$ increases, the stability domain reduces [10].

4.1.1. *Rectangular mesh*

A way to represent this stability domain is to obtain numerically the maximum values of the time-step and the correction parameter $(\Delta t, \alpha)$, such that the condition (16) may be verified. We represent on figure 2 the stability domains obtained for different values of $h = \Delta x = \Delta y$. The optimum value α_{opt} is the one from which Δt remains constant.

We note that the optimum value α_{opt} decreases when the mesh-step h increases : it means that for coarse grids, the influence of the viscosity term is more important. We give in Table 1 the values α_{opt} obtained for different values of h.

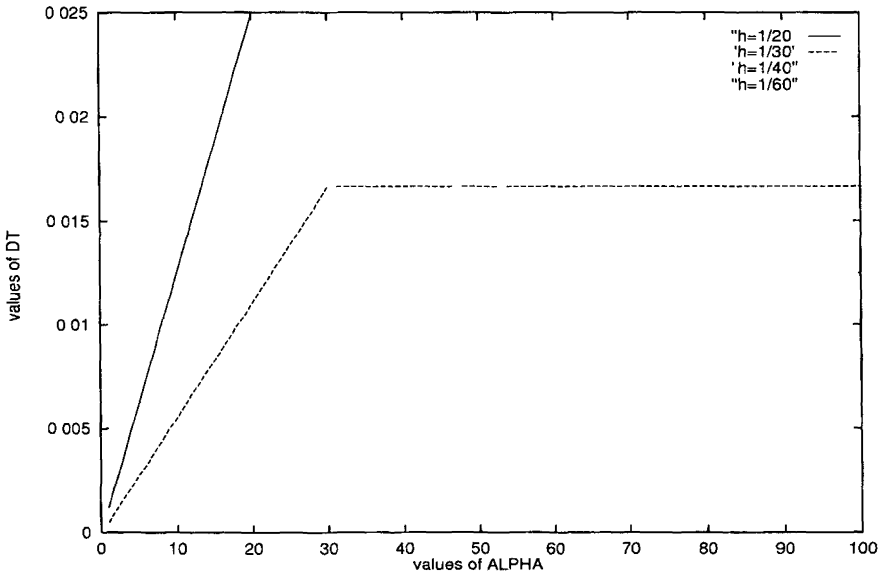

Figure 2. — Stability domain for different values of h.

Table 1.

h	$\Delta t_{\max}$	α_{opt}
1/20	$2.5\ 10^{-2}$	20
1/30	$1.66\ 10^{-2}$	30
1/40	$1.25\ 10^{-2}$	40
1/60	$8.33\ 10^{-3}$	60
1/250	$2\ 10^{-3}$	250

If we choose $\alpha = \alpha_{opt}$, then the stability study [4] allows us to express the maximum time-step $\Delta t_{\max}$ with respect to h :

$$\Delta t_{\max} = \frac{h}{2}.$$

We numerically observe (see table 1) that the viscosity coefficient ($1/\alpha_{opt}$) is related to the mesh-step h and can be expressed into :

$$\text{for} \quad h \leqslant \frac{1}{20}, \quad \alpha_{opt} = \frac{1}{h} = \frac{1}{2\,\Delta t_{\max}}.$$

4.1.2. *Triangular mesh*

We represent on figure 3 the stability domains with respect to Δt and α for different values of $h = \Delta x = \Delta y$, in the case of a structured triangular mesh.

We notice on figure 3, that for a fixed value of h, the maximum time-step $\Delta t_{\max}$ is higher that the one obtained in the rectangular case. It comes from the fact that, for a rectangular grid, the stability limit is the most restrictive in the case of a square grid $\Delta x = \Delta y$ [4].

We also note that, for a fixed value of h or Δt, the value of α_{opt} is higher in the case of a triangular mesh.

Table 2.

h	$\Delta t_{\max}$	α_{opt}
1/15	$4.4\ 10^{-2}$	45
1/20	$3.3\ 10^{-2}$	60
1/30	$2.2\ 10^{-2}$	90
1/40	$1.6\ 10^{-2}$	120
1/60	$9\ 10^{-3}$	145

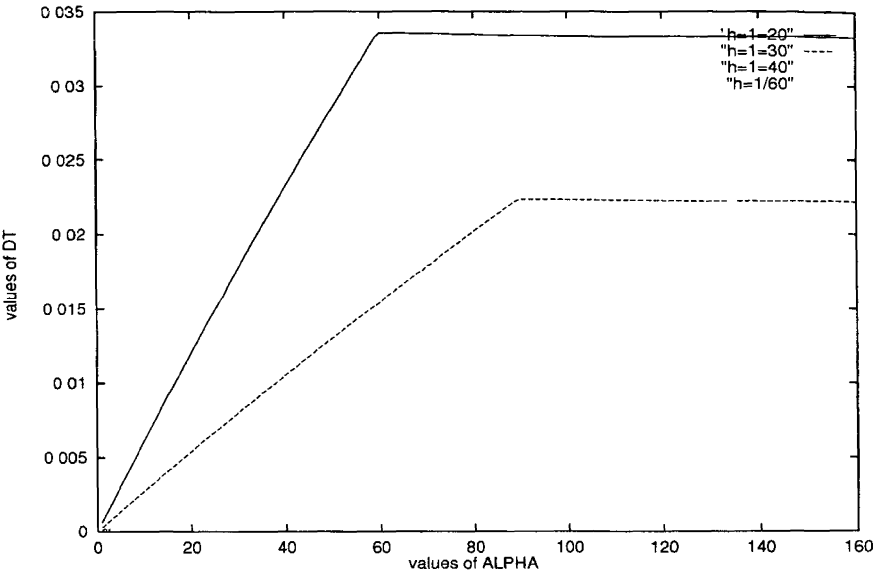

Figure 3. — Stability domains for different values of h.

As for the rectangular mesh, the viscosity coefficient ($1/\alpha_{opt}$) varies linearly with h :

$$\text{for} \quad h \leqslant \frac{1}{15}, \quad \alpha_{opt} = \frac{3}{h}$$

4.2. β-schemes

We consider a Runge-Kutta three-step method and we introduce the following characteristic polynom :

$$g(z) = 1 + z + \frac{z^2}{2} + \frac{z^3}{6}.$$

For $z = A\,\Delta t$, one recalls that the polynom $G(A\,\Delta t)$ represents the amplification matrix of the Runge-Kutta method, applied to the integration of

the differential system $Q_t = AQ$, where A is the 3×3 scheme matrix. Using the notations introduced before and Fourier analysis leads to :

$$\hat{Q}^{n+1} = G_{\theta_1, \theta_2}(A\ \Delta t)\ \hat{Q}^n$$

and Von Neumann theorem (16) still applies to $G_{\theta_1, \theta_2}(A\ \Delta t)$.

4.2.1. *Rectangular mesh*

As we did before, we search for the β-schemes the optimum parameter α_{opt} which allows us to use the same time-step as for the classical Maxwell system. We recall that for $\beta = 0$, we obtain a centered scheme, for $\beta = \frac{1}{2}$ the scheme is half-centered, and $\beta = 1$ gives a fully-upwind scheme.

We represent on figure 4 the stability domains with respect to Δt and α for different values of the upwinding parameter β and for a fixed value of the mesh-step $h = \Delta x = \Delta y = \frac{1}{20}$.

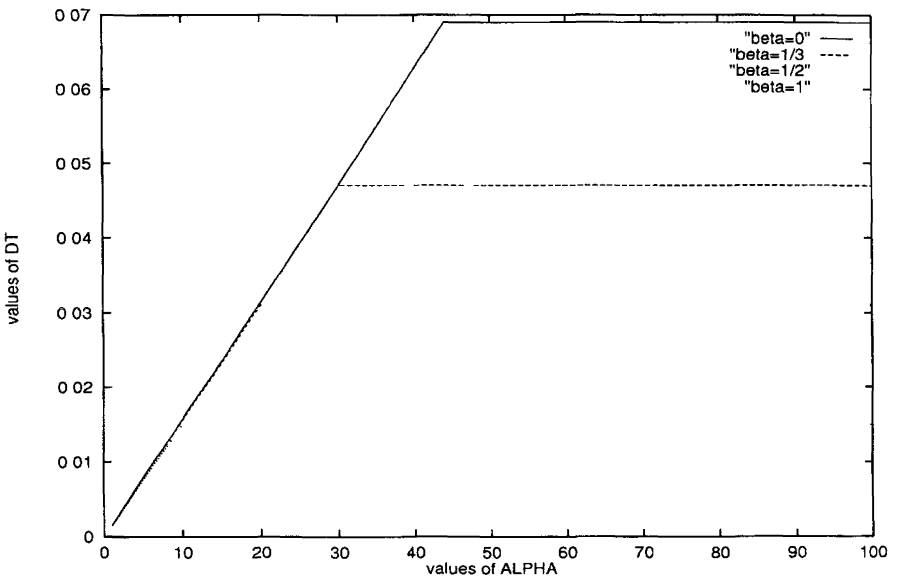

Figure 4. — Stability domains for different values of β

Figure 4 shows that the smaller β is, the higher the stability limit is, which means that using a centered scheme allows us to take a higher time-step. In the same way, when β decreases, the parameter α_{opt} increases : for a fully-centered scheme, the influence of the viscosity term is less important than for an upwind scheme.

We summarize in Table 3 the values of α_{opt} computed for different values of β.

Table 3.

β	$\Delta t_{\max}$	α_{opt}
0	$6.9\ 10^{-2}$	45
1/3	$4.7\ 10^{-2}$	30
1/2	$3.1\ 10^{-2}$	20
1	$1.5\ 10^{-3}$	10

Now we represent on figure 5 the stability domains with respect to Δt and α, for different values of the mesh-step $h = \Delta x = \Delta y$, and for a fixed value of β. In order to have a third-order accurate scheme, we set $\beta = \frac{1}{3}$.

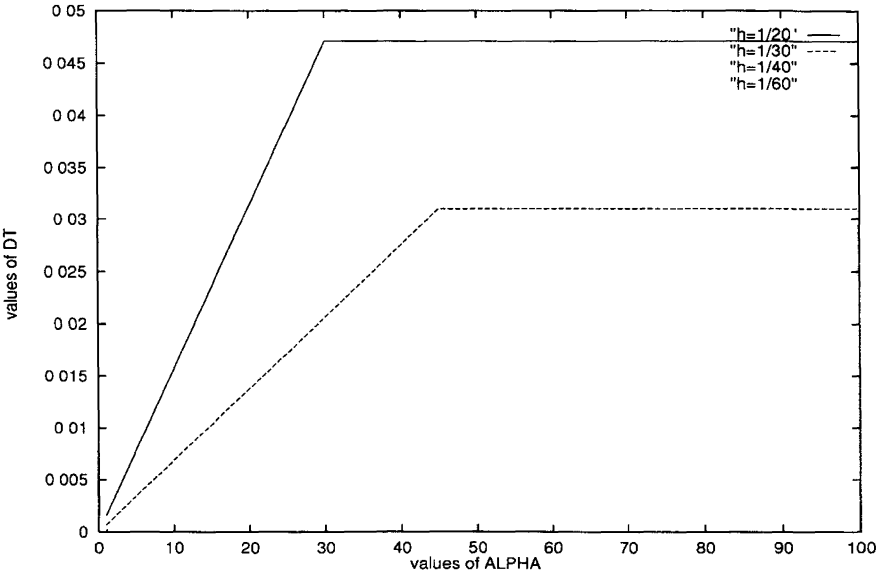

Figure 5. — Stability domains for different values of h.

The stability domains on figure 5 vary in the same way as they do for a first-order accurate scheme (see *fig.* 2) : for a fixed value of Δt, the more h increases, the more α_{opt} decreases and the more important the influence of the viscosity term is.

Table 4.

h	$\Delta t_{\max}$	α_{opt}
1/20	$4.7\ 10^{-2}$	30
1/30	$3.1\ 10^{-2}$	45
1/40	$2.3\ 10^{-2}$	60
1/50	$1.8\ 10^{-2}$	75
1/60	$1.5\ 10^{-2}$	90

As for first-order schemes, the viscosity parameter varies linearly with respect to h and satisfies the relation :

$$\text{for} \quad h \leqslant \frac{1}{20}, \quad \alpha_{opt} = \frac{3}{2h}$$

4.2.2. *Triangular mesh*

As we did with the rectangular mesh (see *fig.* 4), we fix here the mesh-step $h = \frac{1}{20}$, and we represent on figure 6 the stability domains with respect to Δt and α, for different values of β.

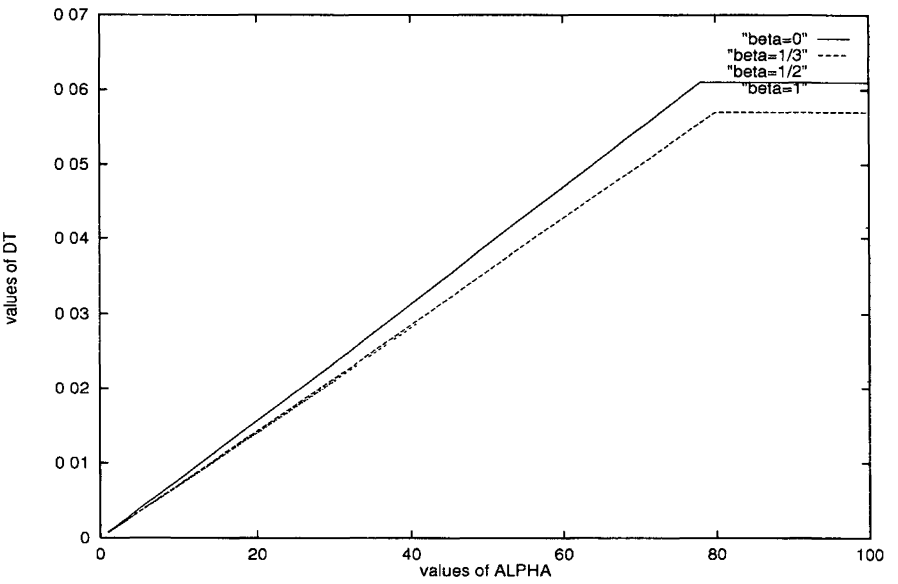

Figure 6. — Stability domains for different values of β

Figures 4 and 6 show that the stability domains vary in the same way with β for rectangular and triangular meshes. For a fixed value of β, we note that the maximum time-step is higher for a triangular mesh, except when the scheme is fully-centered ($\beta = 0$). For a fixed value of β and for a same time-step Δt, the value of α_{opt} is smaller when considering a rectangular mesh. The values α_{opt} in this case do not vary linearly with β.

Table 5.

β	$\Delta t_{\max}$	α_{opt}
0	$6.1\ 10^{-2}$	78
1/3	$5.7\ 10^{-2}$	80
1/2	$4.1\ 10^{-2}$	58
1	$2.1\ 10^{-2}$	30

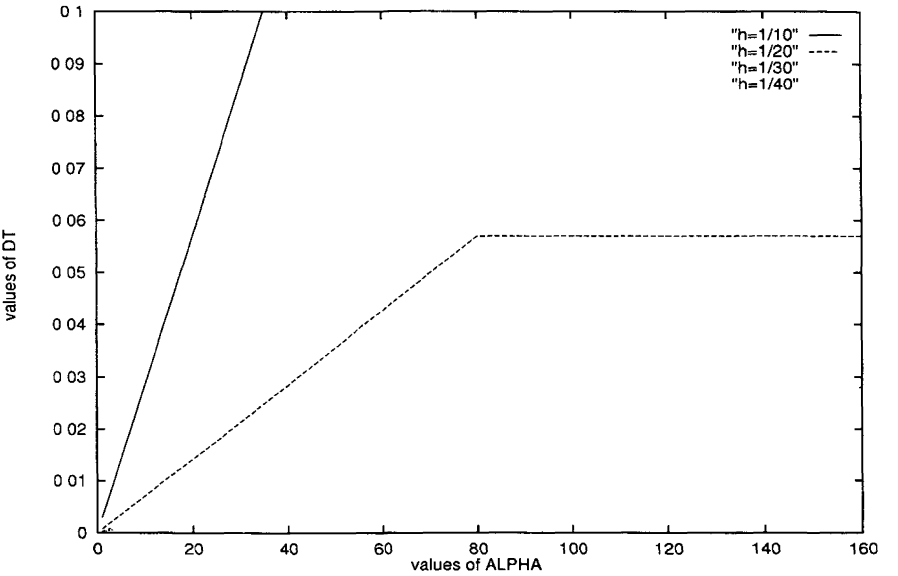

Figure 7. — Stability domains for different values of h.

For the value $\beta = \frac{1}{3}$, we represent on figure 7 the stability domains with respect to Δt and α for different values of $h = \Delta x = \Delta y$.

For a fixed value of h, the maximum time-step that we can choose is still higher for a triangular mesh. However, the ratio $\frac{\Delta t_{RK3}}{\Delta t_{RK1}}$ is 1.8 for a rectangular mesh and 1.7 for a triangular one.

Table 6.

h	$\Delta t_{\max}$	α_{opt}
1/20	$5.7\ 10^{-2}$	80
1/30	$3.8\ 10^{-2}$	120
1/40	$2.8\ 10^{-2}$	160
1/50	$2.2\ 10^{-2}$	200

As for first-order schemes, the viscosity coefficient ($1/\alpha_{opt}$) is related to h by a linear law :

$$\text{for} \quad h \leqslant \frac{1}{10}, \quad \alpha_{opt} = \frac{4}{h}$$

To sum up, this stability study allows us to find an optimum parameter α_{opt} which depends on the meshes and the accuracy of the schemes. We can see that the use of a triangular mesh in the case $\Delta x = \Delta y$ gives us the highest time-step. We note that, for all schemes seen previously, the viscosity coefficient ($1/\alpha_{opt}$) always varies linearly with h. We can see on figure 8 the influence of this parameter with respect to h, for the different schemes. The value of the diffusion coefficient is the highest one for first-order accurate schemes using a rectangular mesh.

5. MODIFIED EQUATIONS

The modified equations technique, introduced by Warming and Hyett [16], allows a detailed analysis of the truncation error of the numerical methods ; in particular the dissipative or the dispersive effect of each error term.

In order to obtain these equations, we apply the new method presented in [2] to the constrained Maxwell system (13.3, 13.4). This method is much simpler for linear constant-coefficients numerical methods, and has the advantage of keeping the same simplicity for multi-step schemes, like Runge-Kutta methods, and for any space dimensions. For more details on this method, one may refer to [2].

In this part, we shall establish the modified equations of the schemes seen previously, concerning the magnetic and the electric fields, but also for the electric field divergence.

5.1. Modified equations for first-order schemes

5.1.1 Rectangular mesh

We recall that we now consider the case of a **TE** wave. The modified equation is written for the first component E^1 of the electric field, since the

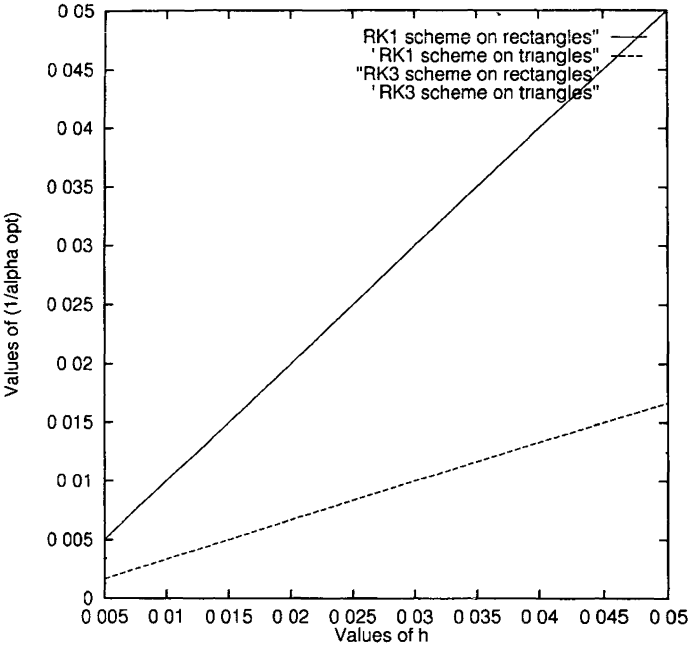

Figure 8. — Representation of the optimum viscosity term with respect to h.

modified equations of the other components can be easily deduced from (17). The value $\alpha = \infty$ gives the modified equation of the scheme applied to the classical Maxwell system In the following we will denote $\frac{\partial^{n+m} E^k}{\partial x^n \partial y^m}$ $k = 1, 2$ by $E^k_{nx\, my}$ In the case $\alpha < \infty$, one obtains :

$$E^1_t + B^3_y = \frac{1}{2}(\Delta y - \Delta t) E^1_{2y} + \left(\frac{\Delta t}{2} + \frac{1}{\alpha}\right) E^1_{xy}$$

$$+ \frac{E^1_{2x}}{\alpha} - \frac{\Delta t}{2\alpha^2}(E^1_{4x} + E^1_{2x2y} + E^2_{x3y} + E^2_{3xy})$$

$$+ O(\Delta t, \Delta x, \Delta y)^2 \qquad (17)$$

We note that the constrained method consists in adding two-order and four-order dissipative terms

$$\left(\frac{E^1_{2x}}{\alpha}, \frac{E^2_{xy}}{\alpha}\right) \quad \text{and} \quad \left(-\frac{\Delta t}{2\alpha^2}(E^1_{4x} + E^1_{2x2y} + E^2_{x3y} + E^2_{3xy})\right).$$

We establish now the modified equations for the divergence in order to prove the efficiency of the constrained formulation to reduce the error on the divergence conditions. It is easily derived from the modified equations of the electric field **E**.

$$
\begin{aligned}
(\operatorname{div}\mathbf{E})_t &= E^1_{tx} + E^2_{ty} \\
&= \frac{\Delta y}{2} E^1_{x2y} + \frac{\Delta y}{2} E^2_{2xy} + \frac{E^2_{3y}}{\alpha} + \frac{E^1_{x2y}}{\alpha} + \frac{E^1_{3x}}{\alpha} + \frac{E^2_{3xy}}{\alpha} \\
&\quad - \frac{\Delta t}{2\alpha^2}(E^1_{5x} + 2E^1_{3x2y} + E^1_{x4y} + E^2_{5y} + E^2_{2x3y} + E^2_{4xy}) \\
&\quad + O(\Delta t, \Delta x, \Delta y)^2
\end{aligned}
$$

which can transform into :

$$
\begin{aligned}
(\operatorname{div}\mathbf{E})_t - \frac{1}{\alpha}\Delta \operatorname{div}\mathbf{E} + \frac{\Delta t}{2\alpha^2}\Delta^2 \operatorname{div}\mathbf{E} \\
= \frac{\Delta y}{2} E^1_{x2y} + \frac{\Delta x}{2} E^2_{2xy} + O(\Delta t, \Delta x, \Delta y)^2 \qquad (18)
\end{aligned}
$$

where $\Delta^2 \operatorname{div}\mathbf{E} = \Delta \circ \Delta(\operatorname{div}\mathbf{E})$. We clearly observe that the constrained method consists in adding more of diffusion on the divergence of **E**.

5.1.2. *Triangular mesh*

As for the rectangular case, we shall establish the modified equations of the first-order scheme. For the sake of simplicity in the calculation, let us set $h = \Delta x = \Delta y$.

The modified equation for the first component of the electric field writes as :

$$
\begin{aligned}
E^1_t + B^3_y &= \left(\frac{ah}{6} + \frac{1}{\alpha}\right) E^1_{2x} + \left(\frac{ah}{6} - \frac{\Delta t}{2}\right) E^1_{2y} + \frac{h}{3\sqrt{2}} E^1_{xy} \\
&\quad + \frac{bh}{6}(E^2_{2x} + E^2_{2y}) + \left(-\frac{h}{3\sqrt{2}} + \frac{\Delta t}{2} + \frac{1}{\alpha}\right) E^2_{xy} \\
&\quad - \frac{\Delta t}{2\alpha^2}(E^1_{4x} + E^1_{2x2y} + E^2_{x3y} + E^2_{3xy}) + O(\Delta t, h)^2
\end{aligned}
$$

where

$$
a = \frac{1}{\sqrt{2}} + \frac{1}{\sqrt{5}}, \quad b = \frac{2}{\sqrt{5}} - \frac{1}{\sqrt{2}}, \quad c = \sqrt{2} + \sqrt{5}\,.
$$

We note that time error terms are the same for both first-order schemes. On the contrary, spatial error terms are different and depend on the spatial numerical approximation : the number of first-order error terms is much more important in the case of triangular meshes. Schemes using triangular meshes are generally more dissipative.

Here we give the modified equation for the divergence of the electric field :

$$
\begin{aligned}
&(\operatorname{div}\mathbf{E})_t - \frac{1}{\alpha}\Delta \operatorname{div}\mathbf{E} + \frac{\Delta t}{2\alpha^2}\Delta^2 \operatorname{div}\mathbf{E} \\
&\quad = \frac{h}{6\sqrt{2}}\left(E^1_{3x} + E^1_{2xy} + E^1_{3y} - E^1_{x2y} - E^2_{3x} + E^2_{3y} + E^2_{x2y} - E^2_{2xy}\right) \\
&\quad = \frac{h}{6\sqrt{5}}\left(E^1_{3x} + 2E^1_{2xy} + 2E^1_{3y} + E^1_{x2y} + 2E^2_{3x} + E^2_{3y} + 2E^2_{x2y} - E^2_{2xy}\right) \\
&\qquad + O(\Delta t, h)^2 . \qquad (19)
\end{aligned}
$$

As for the rectangular mesh, the constrained method consists in adding more of diffusion on the divergence. In the right-hand side, the error terms due to the numerical scheme are first-order spatial error terms, which include all the third space derivatives of **E.** These terms come from the spatial diffusion of the numerical scheme.

5.2. Modified equations for β-schemes

In this section we shall establish the modified equations for second and third-order accurate schemes.

5.2.1. *Rectangular mesh*

The modified equation for the first component E^1 writes :

$$
\begin{aligned}
E^1_t + B^3_y = &-\frac{\Delta y^2}{6}(1-3\beta)B^3_{3y} - \frac{\beta}{4}\left(E^1_{4y}\Delta y^3 + E^1_{2x2y}\Delta x^2\Delta y\right) \\
&- \frac{\Delta t^3}{24}\left(E^1_{4y} + E^1_{2x2y} - E^2_{x3y} - E^2_{3xy}\right) + \frac{E^1_{2x}}{\alpha} + \frac{E^2_{xy}}{\alpha} \\
&+ \frac{1}{12\alpha}\left(E^1_{4x}\Delta x^2 + 2E^1_{2x2y}\Delta y^2 + 2E^2_{3xy}\Delta x^2 + 2E^2_{x3y}\Delta y^2\right) \\
&- \frac{\Delta t^3}{24\alpha^4}\left(E^1_{8x} + 3E^1_{6x2y} + 3E^1_{4x4y} + E^1_{2x6y} + E^2_{7xy}\right) \\
&+ 3E^2_{5x3y} + 3E^2_{4x4y} + E^2_{6x2y}) + O(\Delta t, \Delta x, \Delta y)^4 .
\end{aligned}
$$

We have observed with the stability study that the viscosity parameter $(1/\alpha_{opt})$ varies linearly with the mesh-step h. Two values of the upwinding parameter β are interesting for the accuracy of the schemes : the value $\beta = \frac{1}{3}$ allows us to eliminate the spatial dispersive error terms whereas the value $\beta = 0$ has the advantage to make some spatial dissipative terms vanish.

Choosing $\beta = \frac{1}{3}$ and $\alpha = \alpha_{opt}$ gives a third-order accurate scheme in time and space. The error terms due to our constrained method, factor of $\frac{\Delta x^2}{\alpha}$, $\frac{\Delta y^2}{\alpha}$ and $\frac{\Delta t^3}{24\,\alpha^4}$, come from the fourth and the eighth spatial derivatives of **E**.

For the sake of simplicity, we give the modified equation of the divergence in the particular case : $h = \Delta x = \Delta y$.

$$(\operatorname{div}\mathbf{E})_t - \frac{1}{\alpha}\Delta \operatorname{div}\mathbf{E} - \frac{h^2}{6\,\alpha}\Delta^2 \operatorname{div}\mathbf{E} + \frac{h^2}{12\,\alpha}(E^1_{5x} + E^2_{5y}) + \frac{\Delta t^3}{24\,\alpha^4}\Delta^4 \operatorname{div}\mathbf{E} = -\frac{h^2}{6}(1 - 3\beta)(B^3_{x3y} - B^3_{3xy}) - \frac{\beta h^3}{4}(E^1_{x4y} + E^2_{4xy} + E^1_{3x2y} + E^2_{2x3y}) + (\Delta t, h)^4 \qquad (20)$$

where $\Delta^4 \operatorname{div}\mathbf{E} = \Delta\circ\Delta\circ\Delta\circ\Delta\,(\operatorname{div}\mathbf{E})$.

For the value $\alpha = \alpha_{opt}$, we note that the divergence error is second-order accurate in space, except for $\beta = \frac{1}{3}$ where it is third-order accurate. In this case, the error terms come from the spatial dissipative terms of the scheme.

We can see that the error terms due to the constrained method still add some dissipation on the divergence of **E**.

5.2.2. *Triangular mesh*

We now establish the modified equation for the β-scheme using a triangular mesh, in the case $h = \Delta x = \Delta y$.

$$E^1_t + B^3_y = -\frac{h^2}{6}(1 - 3\beta)(B^3_{3y} + B^3_{2xy} + B^3_{x2y}) - \beta h^3 g(\ldots) - \frac{\Delta t^3}{24}(E^1_{4y} + E^1_{2x2y} - E^2_{x3y} - E^2_{3xy}) + \frac{E^1_{2x}}{\alpha} + \frac{E^2_{xy}}{\alpha} + \frac{1}{12\,\alpha}(E^1_{4x}\Delta x^2 + 2\,E^2_{3xy}\Delta x^2 + 2\,E^2_{x3y}\Delta y^2) - \frac{\Delta t^3}{24\,\alpha^4}(E^1_{8x} + 3\,E^1_{6x2y} + 3\,E^1_{4x4y} + E^1_{2x6y} + E^2_{7xy} + 3\,E^2_{5x3y} + 3\,E^2_{4x4y} + E^2_{6x2y}) + O(\Delta t, h)^4 .$$

where g depends linearly on the fourth spatial derivatives of E^1 and E^2.

As for the rectangular mesh, the value $\beta = \frac{1}{3}$ allows to eliminate the spatial dispersive terms ; we also note that the error terms are more important for a triangular mesh ; for instance we can find some dispersive terms like B^3_{xxy}, B^3_{xyy} and also some dissipative terms in g like E^1_{xxxy}, E^2_{xyyy}. We note again that time error terms keep the same coefficients for triangular and rectangular meshes.

As for first-order schemes, β-schemes using a triangular mesh are more dissipative : indeed the numerical approximation for a triangular mesh needs 19 nodes of calculation whereas a β-scheme using a rectangular mesh has only 9 nodes of calculation.

The error terms due to the constrained method are time and space dissipative terms.

The modified equation for the divergence of **E** writes, in the case $h = \Delta x = \Delta y$:

$$(\operatorname{div} \mathbf{E})_t - \frac{1}{\alpha} \Delta \operatorname{div} \mathbf{E} - \frac{h^2}{6\alpha} \Delta^2 \operatorname{div} \mathbf{E} + \frac{h^2}{12\alpha} (E^1_{5x} + E^2_{5y} + 2 E^1_{3x2y} + 2 E^2_{2x3y}) + \frac{\Delta t^3}{24 \alpha^4} \Delta^4 \operatorname{div} \mathbf{E} = -\beta h^3 k(\,.\,,\,.\,) + O(\Delta t, h)^4 \tag{21}$$

where k depends linearly on the fifth space derivatives of the components E^1 and E^2. In the particular case $h = \Delta x = \Delta y$, the error terms coming from the dispersion of the schemes vanish. In this case, the divergence error, for the value $\alpha = \alpha_{opt}$, is third-order accurate in time and space.

We still notice that the constrained terms are in fact dissipative terms for the divergence.

As a conclusion, we have proved using the modified equations that the divergence error was very sensitive to the spatial accuracy of the scheme : indeed, the error terms on the divergence come from the dispersive and the dissipative effects of the spatial approximation. The constrained method that we proposed here consists in increasing the dissipation of the schemes in order to improve the numerical verification of the divergence conditions (1.3, 1.4).

6. NUMERICAL RESULTS

In this section, we are concerned with the divergence conditions (1.3, 1.4). We will prove that the introduction of a viscosity term in the Maxwell system allows to better satisfy, at the discrete level, the divergence conditions.

Without charges

We consider the system (13.3, 13.4) in two space dimensions for a transverse electric **TE** wave on $\Omega =]0, 1[\times]0, 1[$ with periodic boundary

conditions. We initialize the electromagnetic field with a linear combination of sinusoidal waveforms at different frequencies.

On figures 9 and 10, we present $\| \operatorname{div} \mathbf{E} \|_{L^1(\Omega)}$ in function of time for a fixed mesh-step $h = \Delta x = \Delta y$ and for different values of the parameter α. We consider first and third-order schemes on a rectangular mesh.

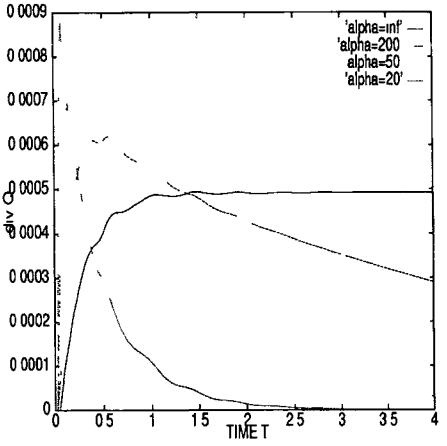

Figure 9. — First-order scheme.

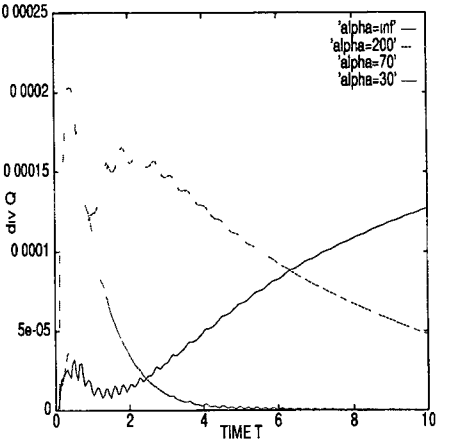

Figure 10. — Third-order scheme.

On figures 11 and 12, we present the same quantities for a triangular mesh.

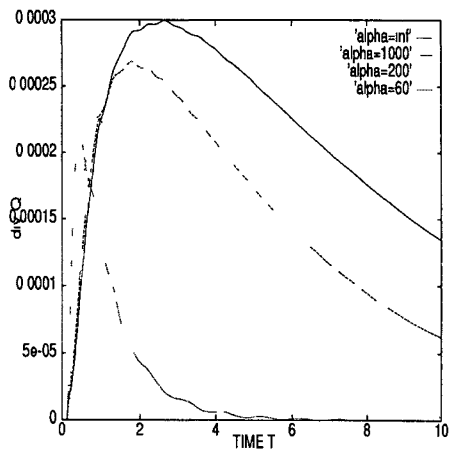

Figure 11. — First-order scheme.

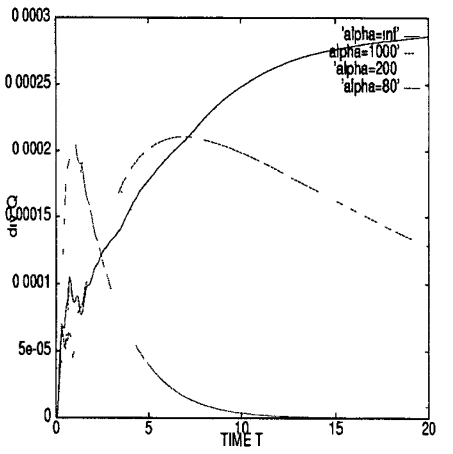

Figure 12. — Third-order scheme.

When the parameter α decreases, which corresponds to a greater influence of the viscosity terms in (13.1, 13.2), the divergence of the electric field is smaller. However, the constraint on the time step Δt becomes more important

for stability reasons. Nevertheless, we have shown previously the existence of an optimum value α_{opt} which introduces any additional constraint on Δt. We note also that $\mathrm{div}_h \mathbf{E} \to 0$ when t goes to infinity. We compare now the influence of the mesh (rectangles or triangles) on the divergence of the electric field **E**.

We present on figures 13 and 14, $\| \mathrm{div}\, \mathbf{E} \|_{L^1(\Omega)}$ in function of time for a fixed $h = \Delta x = \Delta y$ with the optimal value α_{opt} for first and third-order schemes.

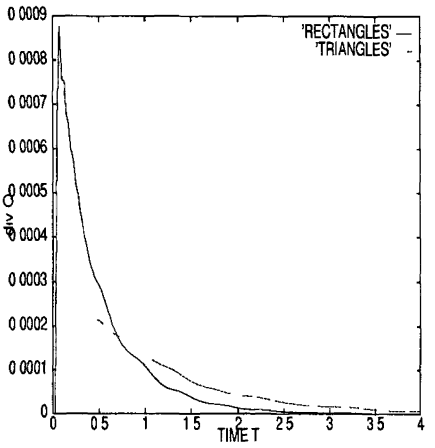

Figure 13. — First-order scheme.

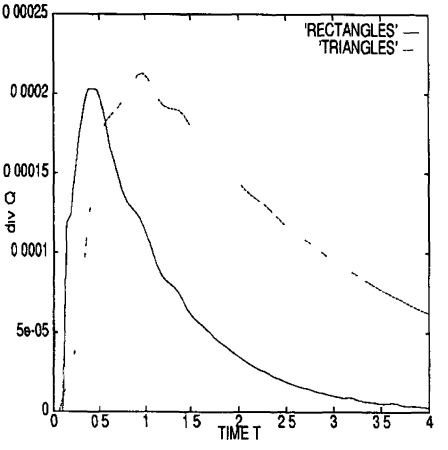

Figure 14. — Third-order scheme.

We remark that $\| \mathrm{div}\, \mathbf{E} \|_{L^1(\Omega)}$ is smaller when we consider a rectangular mesh, for first and third-order schemes. Indeed, the optimal value α_{opt} is smaller for the scheme in rectangles, therefore the influence of the viscosity term is more important. Nevertheless, we can use larger time-steps for triangular meshes which allows to decrease the time cost. We study now the influence of the upwinding parameter β on the divergence of the electric field **E**.

We present on figures 15 and 16 $\| \mathrm{div}\, \mathbf{E} \|_{L^1(\Omega)}$ in function of time for a fixed value of $h = \Delta x = \Delta y$. We use the optimum value α_{opt} for the different values of β, on rectangular and triangular meshes.

We recall that for $\beta = 0$, the scheme is centered and for $\beta = 1$ we obtain a fully-upwind scheme. We remark, for the two schemes, that the divergence error decreases when β increases. Nevertheless, the constraint on the time-step Δt increases with β. We can conclude that the best choice for β is $\beta = 1/3$, in this case the divergence is small, the constraint on the time-step is not important and the scheme is third-order accurate in space.

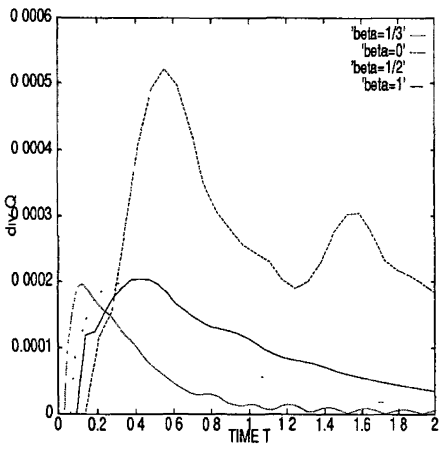

Figure 15. — Rectangular meshes.

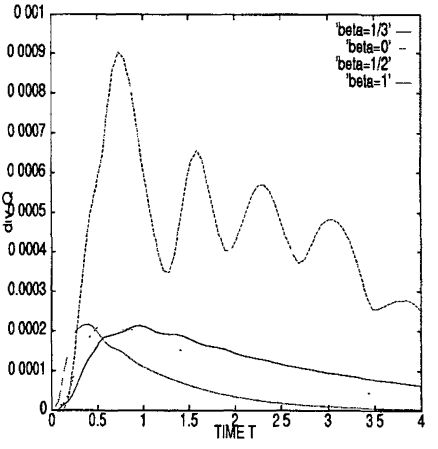

Figure 16. — Triangular meshes.

Now, we are interested in the influence of the viscosity terms on the electromagnetic field. We consider a **TE** wave solution of the Maxwell system :

$$\begin{cases} E_x(t,x,y) &= -\cos\left(x+y-\sqrt{2}\,t\right) \\ E_y(t,x,y) &= \cos\left(x+y-\sqrt{2}\,t\right) \\ B_x(t,x,y) &= \sqrt{2}\cos\left(x+y-\sqrt{2}\,t\right). \end{cases}$$

We present on figures 17 and 18, $\|\mathbf{B}-\mathbf{B}_h\|_{L^\infty(\Omega)}$ in function of time for different values of α and $h = \Delta x = \Delta y$, for first and third-order schemes using a triangular mesh.

We note that the introduction of a viscosity term in the Maxwell system does not involve an important additional error on the electromagnetic field. The addition of a viscosity term in the Maxwell system is equivalent, at the discrete level, to add some diffusion in our schemes. One can also notice the great influence of the mesh thickness on the accuracy of the electromagnetic field.

In presence of charges

Given the following charge and current densities :

$$\begin{cases} \rho(t,x,y) = \sin(t) * (\sin(\pi y) + \sin(\pi x)) \\ j_x(t,x,y) = (\cos(t)-1)(\pi\cos(\pi x) + \pi^2 x \sin(\pi y)) - x\cos(t)\sin(\pi y) \\ j_y(t,x,y) = (\cos(t)-1)(\pi\cos(\pi y) + \pi^2 y \sin(\pi x)) - y\cos(t)\sin(\pi x). \end{cases}$$

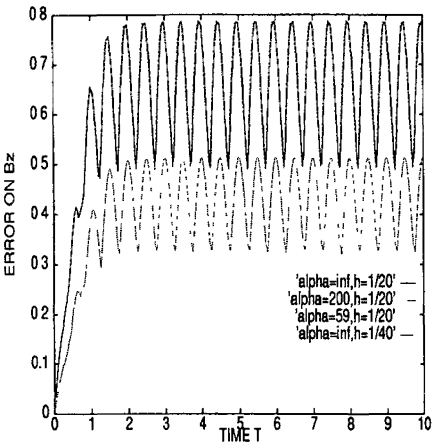

Figure 17. — First-order scheme.

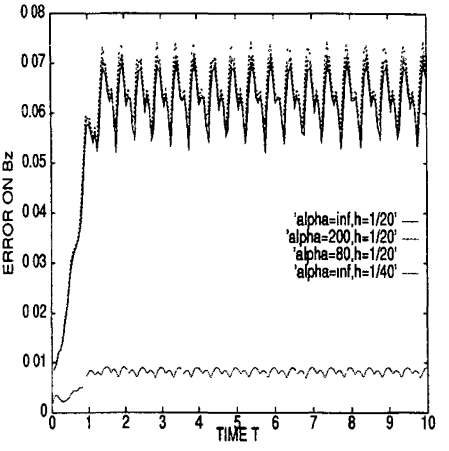

Figure 18. — Third-order scheme.

We consider the problem (13.3, 13.4) on a bounded domain $\Omega =]0, 1[\times]0, 1[$. We supplement the problem (13.3, 13.4) with initial conditions

$$E_0^x(x, y) = 0, \quad E_0^y(x, y) = 0, \quad B_0^x(x, y) = 0$$

and boundary conditions. The boundary $\Gamma = \partial\Omega$ is assumed to be perfectly conducting : $\mathbf{n} \times \mathbf{E} = 0$ on Γ. We can determine the exact solution of the problem (13.3, 13.4) with such initial and boundary conditions. The exact solution is given by :

$$\mathbf{E} = \sin(t) \begin{pmatrix} x \sin(\pi y) \\ y \sin(\pi x) \\ 0 \end{pmatrix}$$

$$\mathbf{B} = (\cos(t) - 1) \begin{pmatrix} 0 \\ 0 \\ \pi y \cos(\pi x) - \pi x \cos(\pi y) \end{pmatrix}.$$

We consider here the third-order scheme for a triangular mesh. We present on figures 19 and 20, $\| \operatorname{div} \mathbf{E} - \rho \|_{L^1(\Omega)}$ and $\| \mathbf{E} - \mathbf{E}_h \|_{L^1(\Omega)}$ in function of time, for different values of the mesh step $h = \Delta x = \Delta y$ and for a fixed value of the coefficient α.

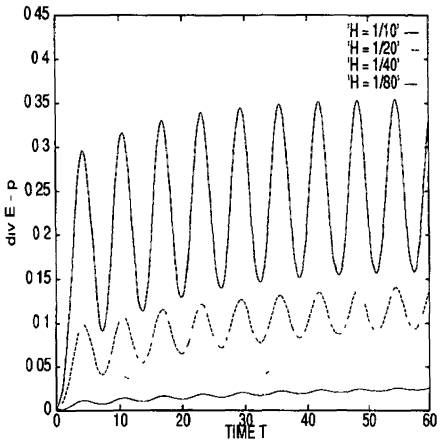

Figure 19. — div $\mathbf{E}_h - \rho$ with respect to h.

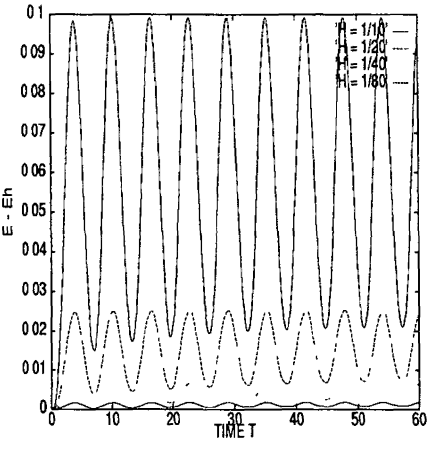

Figure 20. — $\mathbf{E} - \mathbf{E}_h$ with respect to h.

One can notice the great influence of the mesh thickness on the electromagnetic field and on the divergence.

We present now, for the third-order scheme using a triangular mesh, on figure 21 $\| \operatorname{div} \mathbf{E}_h - \boldsymbol{\rho} \|_{L^1(\Omega)}$ in function of time for different values of the coefficient α and for a fixed value of the mesh step $h = \Delta x = \Delta y$. On figure 22, we present $\| \operatorname{div} \mathbf{E}_h - \boldsymbol{\rho} \|_{L^1(\Omega)}$ in function of time, for $h = \frac{1}{40}$ with the optimal value of α, and for $h = \frac{1}{80}$ with $\alpha = \infty$ (for $\alpha = \infty$ we recover the classical formulation of the Maxwell system).

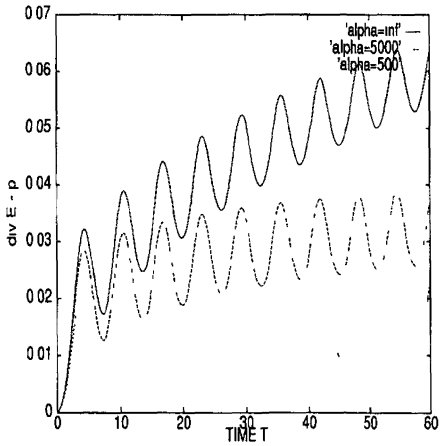

Figure 21. — div $\mathbf{E}_h - \rho$ with respect to α.

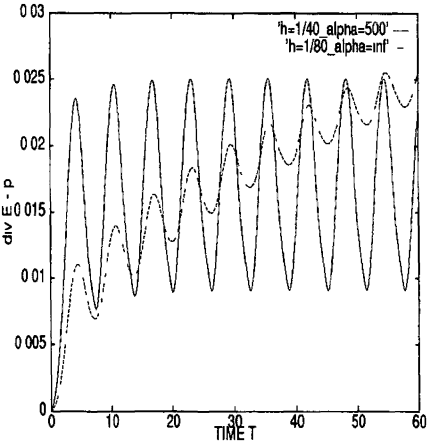

Figure 22. — div $\mathbf{E}_h - \boldsymbol{\rho}$ with respect to α and h.

We notice that when the value of α decreases (which corresponds to a greater influence of the viscosity terms), the relation (1 3) is better satisfied We remark on figure 34, that the divergence error is of the same order for a given mesh step h using the new formulation of the Maxwell system than for a mesh step $h/2$ using the classical Maxwell system

We compare now on figure 23, $\| \operatorname{div} \mathbf{E}_h - \rho \|_{L^1(\Omega)}$ for the first and third-order schemes, for fixed values of $h = \Delta x = \Delta y$ and α The amplitude is reduced by a factor ten when comparing a first order and a quasi third-order scheme in space One can conclude that the accuracy of the scheme has a freat influence on the relation (1 3)

Computational cost

It is interesting to evaluate the cost, in terms of CPU time, involved by the introduction of a viscosity term in the Maxwell system The resolution of the system (13 1, 13 2) requires about 7 % of additional CPU time compared to the resolution of the Maxwell system (1 1, 1 2) The cost in terms of memory storage is about 4 % One can conclude that the method presented improves the numerical verification of the divergence relations (1 3, 1 4) without involving an important additional cost

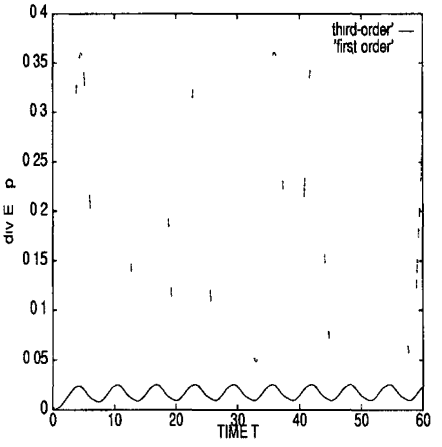

Figure 23. — First-order and third-order schemes.

7. CONCLUSION

We have presented a new constrained formulation for the Maxwell system in order to improve the numerical verification of the divergence conditions (1 3, 1 4) The numerical results that we obtained are very satisfying and this method seems to be well-adapted to the numerical conservation of the divergence

The stability study allows us to find an optimum viscosity parameter which introduces no restriction on the time-step. The value of this parameter depends on the choice of the mesh (rectangular or triangular) and on the accuracy of the scheme.

We also focalise on the modified equation technique, which allows us to obtain the error terms due to the numerical approximation, for the schemes and also for the variation in time of the divergence. Choosing the values $\beta = \frac{1}{3}$ and $\alpha = \alpha_{opt}$ leads to a third-order accurate scheme in time and space, and also to a third-order divergence error, on both rectangular and triangular meshes.

We also not the influence of the mesh-step h on the divergence error : applying our new constrained method to the three-dimensional case would allow to reduce the number of mesh nodes, and therefore to reduce the computational cost, in comparison to the classical Maxwell system.

8. ACKNOWLEDGEMENTS

The authors wish to thank Frédéric Poupaud (University of Nice), Loula Fézoui and Armel de la Bourdonnaye (CERMICS-INRIA) for their fruitful help concerning this work.

REFERENCES

[1] F. ASSOUS, P. DEGOND, J. SEGRÉ, 1992, *A particle-tracking method for 3D electromagnetic PIC codes on unstructured meshes,* Comp. Phys. Comm., **72,** pp. 105-114.

[2] R. CARPENTIER, A. de la BOURDONNAYE, B. LARROUTUROU, 1994, *On the derivation of the modified equation for the analysis of linear numerical methods,* CERMICS Report no. 26.

[3] S. DEPEYRE, R. CARPENTIER, *High-order upwind numerical methods in two space dimensions,* CERMICS Report, to appear.

[4] S. DEPEYRE, *Stability analysis for the finite volume schemes on rectangular and triangular meshes applied to the 2D Maxwell system,* to appear.

[5] J. P. CIONI, L. FEZOUI, H. STEVE, 1993, *A parallel time-domain Maxwell solver using upwind schemes and triangular meshes,* IMPACT in computing in science and engeenering No 165.

[6] J. P. CIONI, L. FEZOUI, D. ISSAUTIER, *High-order upwind schemes for solving time-domain Maxwell equation,* La Recherche Aérospatiale, numéro spécial électromagnétisme.

[7] R. DAUTRAY, J. L. LIONS, 1987, *Analyse mathématique et calcul numérique,* Masson, **1,** 68-127.

[8] J. A. DESIDERI, A. GOUJO, V. SELMIN, 1987, *Third-order numerical schemes for hyperbolic problems,* Rapport de recherche INRIA no. 607.

[9] L. FEZOUI, 1985, *Résolution des équations d'Euler par un schéma de Van Leer en éléments finis,* INRIA Report no. 358.

[10] N. GLINSKY, 1990, *Simulation numérique d'écoulements hypersoniques réactifs hors-équilibre chimique,* Thesis, University of Nice-Sophia-Antipolis.

[11] D. ISSAUTIER, J. P. CIONI, F. POUPAUD, L. FEZOUI, *A 2-D Vlasov-Maxwell solver on unstructured meshes,* Third international conference on mathematical and numerical aspects of wave propagation phenomena, Mandelieu, avril 1995.

[12] P. D. LAX, A. HARTEN, B. Van LEER, 1983, *On upstream differencing and Godunov type schemes for hyperbolic conservation laws,* SIAM Revue, Vol. 25, No 1.

[13] S. LANTERI, 1991, *Simulation d'écoulements aérodynamiques instationnaires sur une architecture massivement parallèle,* Thesis, University of Nice-Sophia-Antipolis.

[14] V. SELMIN, 1987, *Finite element solution of hyperbolic equations ; I : one dimensional case, II : two dimensional case,* INRIA Report no. 655.

[15] B. Van LEER, 1982, *Flux vector splitting for the Euler equations,* Lecture Notes in Physics, Vol. 170, pp. 405-512.

[16] R. F. WARMING, HYETT, 1974, *The modified equation approach to the stability and accuracy analysis of finite-difference methods,* J. Comp. Phys., **14,** (2), p. 159.